PHYSICAL REVIEW LETTERS

Observation of $Z_b(10610)$ and $Z_b(10650)$ Decaying to B Mesons

A. Garmash,[3,47] A. Abdesselam,[57] I. Adachi,[13,10] H. Aihara,[62] D. M. Asner,[49] T. Aushev,[38] R. Ayad,[57] T. Aziz,[58] V. Babu,[58] I. Badhrees,[57,26] A. M. Bakich,[56] P. Behera,[17] V. Bhardwaj,[54] B. Bhuyan,[16] A. Bobrov,[3,47] A. Bondar,[3,47] G. Bonvicini,[67] A. Bozek,[45] M. Bračko,[34,22] T. E. Browder,[12] D. Červenkov,[4] V. Chekelian,[35] A. Chen,[42] B. G. Cheon,[11] K. Chilikin,[37] K. Cho,[27] V. Chobanova,[35] Y. Choi,[55] D. Cinabro,[67] J. Dalseno,[35,59] M. Danilov,[37] N. Dash,[15] Z. Doležal,[4] A. Drutskoy,[37] D. Dutta,[58] S. Eidelman,[3,47] D. Epifanov,[62] H. Farhat,[67] J. E. Fast,[49] T. Ferber,[7] B. G. Fulsom,[49] V. Gaur,[58] N. Gabyshev,[3,47] R. Gillard,[67] Y. M. Goh,[11] P. Goldenzweig,[24] B. Golob,[31,22] T. Hara,[13,10] K. Hayasaka,[40] H. Hayashii,[41] T. Iijima,[40,39] A. Ishikawa,[60] R. Itoh,[13,10] Y. Iwasaki,[13] I. Jaegle,[12] D. Joffe,[25] K. K. Joo,[5] T. Julius,[36] K. H. Kang,[29] E. Kato,[60] T. Kawasaki,[46] D. Y. Kim,[53] J. B. Kim,[28] K. T. Kim,[28] M. J. Kim,[29] S. H. Kim,[11] Y. J. Kim,[27] K. Kinoshita,[6] S. Korpar,[34,22] P. Križan,[31,22] P. Krokovny,[3,47] T. Kuhr,[32] A. Kuzmin,[3,47] Y.-J. Kwon,[69] J. S. Lange,[9] I. S. Lee,[11] C. Li,[36] H. Li,[18] L. Li,[51] L. Li Gioi,[35] J. Libby,[17] D. Liventsev,[66,13] P. Lukin,[3,47] M. Masuda,[61] D. Matvienko,[3,47] K. Miyabayashi,[41] H. Miyata,[46] R. Mizuk,[37,38] G. B. Mohanty,[58] A. Moll,[35,59] T. Mori,[39] R. Mussa,[21] E. Nakano,[48] M. Nakao,[13,10] T. Nanut,[22] Z. Natkaniec,[45] S. Nishida,[13,10] S. L. Olsen,[52] P. Pakhlov,[37] G. Pakhlova,[38] B. Pal,[6] H. Park,[29] T. K. Pedlar,[33] R. Pestotnik,[22] M. Petrič,[22] L. E. Piilonen,[66] C. Pulvermacher,[24] E. Ribežl,[22] M. Ritter,[35] A. Rostomyan,[7] H. Sahoo,[12] Y. Sakai,[13,10] S. Sandilya,[58] T. Sanuki,[60] V. Savinov,[50] O. Schneider,[30] G. Schnell,[1,14] C. Schwanda,[20] Y. Seino,[46] D. Semmler,[9] K. Senyo,[68] I. S. Seong,[12] M. E. Sevior,[36] V. Shebalin,[3,47] C. P. Shen,[2] T.-A. Shibata,[63] J.-G. Shiu,[44] B. Shwartz,[3,47] F. Simon,[35,59] Y.-S. Sohn,[69] E. Solovieva,[38] M. Starič,[22] T. Sumiyoshi,[64] U. Tamponi,[21,65] K. Tanida,[52] Y. Teramoto,[48] K. Trabelsi,[13,10] M. Uchida,[63] S. Uehara,[13,10] T. Uglov,[38] S. Uno,[13,10] C. Van Hulse,[1] P. Vanhoefer,[35] G. Varner,[12] V. Vorobyev,[3,47] M. N. Wagner,[9] C. H. Wang,[43] M.-Z. Wang,[44] P. Wang,[19] Y. Watanabe,[23] K. M. Williams,[66] E. Won,[28] H. Yamamoto,[60] J. Yamaoka,[49] S. Yashchenko,[7] J. Yelton,[8] J. Yook,[69] Y. Yook,[69] C. Z. Yuan,[19] Z. P. Zhang,[51] V. Zhilich,[3,47] V. Zhulanov,[3,47] and A. Zupanc[22]

(Belle Collaboration)

[1]*University of the Basque Country UPV/EHU, 48080 Bilbao*
[2]*Beihang University, Beijing 100191*
[3]*Budker Institute of Nuclear Physics SB RAS, Novosibirsk 630090*
[4]*Faculty of Mathematics and Physics, Charles University, 121 16 Prague*
[5]*Chonnam National University, Kwangju 660-701*
[6]*University of Cincinnati, Cincinnati, Ohio 45221*
[7]*Deutsches Elektronen-Synchrotron, 22607 Hamburg*
[8]*University of Florida, Gainesville, Florida 32611*
[9]*Justus-Liebig-Universität Gießen, 35392 Gießen*
[10]*SOKENDAI (The Graduate University for Advanced Studies), Hayama 240-0193*
[11]*Hanyang University, Seoul 133-791*
[12]*University of Hawaii, Honolulu, Hawaii 96822*
[13]*High Energy Accelerator Research Organization (KEK), Tsukuba 305-0801*
[14]*IKERBASQUE, Basque Foundation for Science, 48013 Bilbao*
[15]*Indian Institute of Technology Bhubaneswar, Satya Nagar 751007*
[16]*Indian Institute of Technology Guwahati, Assam 781039*
[17]*Indian Institute of Technology Madras, Chennai 600036*
[18]*Indiana University, Bloomington, Indiana 47408*
[19]*Institute of High Energy Physics, Chinese Academy of Sciences, Beijing 100049*
[20]*Institute of High Energy Physics, Vienna 1050*
[21]*INFN-Sezione di Torino, 10125 Torino*
[22]*J. Stefan Institute, 1000 Ljubljana*
[23]*Kanagawa University, Yokohama 221-8686*
[24]*Institut für Experimentelle Kernphysik, Karlsruher Institut für Technologie, 76131 Karlsruhe*
[25]*Kennesaw State University, Kennesaw, Georgia 30144*
[26]*King Abdulaziz City for Science and Technology, Riyadh 11442*
[27]*Korea Institute of Science and Technology Information, Daejeon 305-806*
[28]*Korea University, Seoul 136-713*
[29]*Kyungpook National University, Daegu 702-701*
[30]*École Polytechnique Fédérale de Lausanne (EPFL), Lausanne 1015*

212001-1

^{31}*Faculty of Mathematics and Physics, University of Ljubljana, 1000 Ljubljana*
^{32}*Ludwig Maximilians University, 80539 Munich*
^{33}*Luther College, Decorah, Iowa 52101*
^{34}*University of Maribor, 2000 Maribor*
^{35}*Max-Planck-Institut für Physik, 80805 München*
^{36}*School of Physics, University of Melbourne, Victoria 3010*
^{37}*Moscow Physical Engineering Institute, Moscow 115409*
^{38}*Moscow Institute of Physics and Technology, Moscow Region 141700*
^{39}*Graduate School of Science, Nagoya University, Nagoya 464-8602*
^{40}*Kobayashi-Maskawa Institute, Nagoya University, Nagoya 464-8602*
^{41}*Nara Women's University, Nara 630-8506*
^{42}*National Central University, Chung-li 32054*
^{43}*National United University, Miao Li 36003*
^{44}*Department of Physics, National Taiwan University, Taipei 10617*
^{45}*H. Niewodniczanski Institute of Nuclear Physics, Krakow 31-342*
^{46}*Niigata University, Niigata 950-2181*
^{47}*Novosibirsk State University, Novosibirsk 630090*
^{48}*Osaka City University, Osaka 558-8585*
^{49}*Pacific Northwest National Laboratory, Richland, Washington 99352*
^{50}*University of Pittsburgh, Pittsburgh, Pennsylvania 15260*
^{51}*University of Science and Technology of China, Hefei 230026*
^{52}*Seoul National University, Seoul 151-742*
^{53}*Soongsil University, Seoul 156-743*
^{54}*University of South Carolina, Columbia, South Carolina 29208*
^{55}*Sungkyunkwan University, Suwon 440-746*
^{56}*School of Physics, University of Sydney, New South Wales 2006*
^{57}*Department of Physics, Faculty of Science, University of Tabuk, Tabuk 71451*
^{58}*Tata Institute of Fundamental Research, Mumbai 400005*
^{59}*Excellence Cluster Universe, Technische Universität München, 85748 Garching*
^{60}*Tohoku University, Sendai 980-8578*
^{61}*Earthquake Research Institute, University of Tokyo, Tokyo 113-0032*
^{62}*Department of Physics, University of Tokyo, Tokyo 113-0033*
^{63}*Tokyo Institute of Technology, Tokyo 152-8550*
^{64}*Tokyo Metropolitan University, Tokyo 192-0397*
^{65}*University of Torino, 10124 Torino*
^{66}*CNP, Virginia Polytechnic Institute and State University, Blacksburg, Virginia 24061*
^{67}*Wayne State University, Detroit, Michigan 48202*
^{68}*Yamagata University, Yamagata 990-8560*
^{69}*Yonsei University, Seoul 120-749*

We report the analysis of the three-body $e^+e^- \to B\bar{B}\pi^{\pm}$, $B\bar{B}^*\pi^{\pm}$, and $B^*\bar{B}^*\pi^{\pm}$ processes, including the first observations of the $Z_b^{\pm}(10610) \to [B\bar{B}^* + \text{c.c.}]^{\pm}$ and $Z_b^{\pm}(10650) \to [B^*\bar{B}^*]^{\pm}$ transitions that are found to dominate the corresponding final states. We measure Born cross sections for the three-body production of $\sigma(e^+e^- \to [B\bar{B}^* + \text{c.c.}]^{\pm}\pi^{\mp}) = [17.4 \pm 1.6(\text{stat}) \pm 1.9(\text{syst})]$ pb and $\sigma(e^+e^- \to [B^*\bar{B}^*]^{\pm}\pi^{\mp}) = [8.75 \pm 1.15(\text{stat}) \pm 1.04(\text{syst})]$ pb and set a 90% C.L. upper limit of $\sigma(e^+e^- \to [B\bar{B}]^{\pm}\pi^{\mp}) < 2.9$ pb. The results are based on a 121.4 fb^{-1} data sample collected with the Belle detector at a center-of-mass energy near the $\Upsilon(10860)$ peak.

　　Two new charged bottomoniumlike resonances, $Z_b(10610)$ and $Z_b(10650)$, have been observed recently by the Belle Collaboration in $e^+e^- \to \Upsilon(nS)\pi^+\pi^-$, $n = 1, 2, 3$ and $e^+e^- \to h_b(mP)\pi^+\pi^-$, $m = 1, 2$ [1,2]. Analysis of the quark composition of the initial and final states reveals that these hadronic objects have an exotic nature: Z_b should be composed of (at least) four quarks

including a $b\bar{b}$ pair. Several models [3] have been proposed to describe the internal structure of these states. In Ref. [4], it was suggested that $Z_b(10610)$ and $Z_b(10650)$ states might be loosely bound $B\bar{B}^*$ and $B^*\bar{B}^*$ systems, respectively. If so, it is natural to expect the Z_b states to decay to final states with $B^{(*)}$ mesons at substantial rates.

Evidence for the three-body $\Upsilon(10860) \to B\bar{B}^*\pi$ decay has been reported previously by Belle, based on a data sample of 23.6 fb^{-1} [5]. In this analysis, we use a data sample with an integrated luminosity of 121.4 fb^{-1} collected near the peak of the $\Upsilon(10860)$ resonance ($\sqrt{s} = 10.866$ GeV) with the Belle detector [6] at the KEKB asymmetric-energy e^+e^- collider [7]. Note that we reconstruct only three-body $B^{(*)}\bar{B}^{(*)}\pi$ combinations with a charged primary pion. For brevity, we adopt the following notations: the set of $B^+\bar{B}^0\pi^-$ and $B^-B^0\pi^+$ final states is referred to as $BB\pi$; the set of $B^+\bar{B}^{*0}\pi^-$, $B^-B^{*0}\pi^+$, $B^0B^{*-}\pi^+$ and $\bar{B}^0B^{*+}\pi^-$ final states is referred to as $BB^*\pi$; and the set of $B^{*+}\bar{B}^{*0}\pi^-$ and $B^{*-}B^{*0}\pi^+$ final states is denoted as $B^*B^*\pi$. The inclusion of the charge conjugate mode is implied throughout this Letter.

We use Monte Carlo (MC) events generated with EVTGEN [8] and then processed through a detailed detector simulation implemented in GEANT3 [9]. The simulated samples for $e^+e^- \to q\bar{q}$ ($q = u, d, s, c$, or b) are equivalent to 6 times the integrated luminosity of the data and are used to develop criteria to separate signal events from backgrounds, identify types of background events, determine the reconstruction efficiency, and parametrize the distributions needed for the extraction of the signal decays.

B mesons are reconstructed in the following decay channels: $B^+ \to J/\psi K^{(*)+}$, $B^+ \to \bar{D}^{(*)0}\pi^+$, $B^0 \to J/\psi K^{(*)0}$, $B^0 \to D^{(*)-}\pi^+$. We use Belle standard techniques [10] to reconstruct primary particles such as photons, pions, kaons, and leptons. The K^{*0} (K^{*+}) is reconstructed in the $K^+\pi^-$ ($K^0\pi^+$) final state; the invariant mass of the K^* candidate is required to be within 150 MeV/c^2 of the nominal K^* mass [11]. The invariant mass of a $J/\psi \to \ell^+\ell^-$ candidate is required to be within 30 (50) MeV/c^2 for $\ell = e$ (μ), of the nominal J/ψ mass. Neutral (charged) D mesons are reconstructed in the $K^-\pi^+$, $K^-\pi^+\pi^0$, and $K^-\pi^-\pi^+\pi^+$ ($K^-\pi^+\pi^+$) modes. To identify D^* candidates, we require $|M(D\pi) - M(D) - \Delta m_{D^*}| < 3$ MeV/c^2, where $M(D\pi)$ and $M(D)$ are the reconstructed masses of the D^* and D candidates, respectively, and $\Delta m_{D^*} = m_{D^*} - m_D$ is the difference between the nominal D^* and D masses. The mass windows for narrow states quoted above correspond to a $\pm 2.5\sigma$ requirement.

The dominant background comes from $e^+e^- \to c\bar{c}$ continuum events, where true D mesons produced in e^+e^- annihilation are combined with random particles to form a B candidate. This type of background is suppressed using variables that characterize the event topology. Since the momenta of the two B mesons produced from a three-body $e^+e^- \to B^{(*)}B^{(*)}\pi$ decay are low in the center-of-mass (c.m.) frame (below 0.9 GeV/c), the decay products of different B mesons are essentially uncorrelated so that the event tends to be spherical. In contrast, hadrons from continuum events tend to exhibit a back-to-back jet

structure. We use θ_{thr}, the angle between the thrust axis of the B candidate and that of the rest of the event, to discriminate between the two cases. The distribution of $|\cos\theta_{\mathrm{thr}}|$ is strongly peaked near $|\cos\theta_{\mathrm{thr}}| = 1.0$ for $c\bar{c}$ events and is nearly flat for $B^{(*)}B^{(*)}\pi$ events. We require $|\cos\theta_{\mathrm{thr}}| < 0.80$ for the $B \to D^{(*)}\pi$ final states; this eliminates about 81% of the continuum background and retains 73% of the signal events.

We identify B candidates by their reconstructed invariant mass $M(B)$ and momentum $P(B)$ in the c.m. frame. We require $P(B) < 1.35$ GeV/c to retain B mesons produced in both two-body and multibody processes. The $M(B)$ distribution for B candidates is shown in Fig. 1(a). We perform a binned maximum likelihood fit of the $M(B)$ distribution to the sum of a signal component parametrized by a Gaussian function and two background components: one related to other decay modes of B mesons and one due to continuum $e^+e^- \to q\bar{q}$ processes, where $q = u, d, s, c$. The shape of the B-related background is determined from a large sample of generic MC simulations, and the shape of the $q\bar{q}$ background is parametrized with a linear function. The parameters of the signal Gaussian, the normalization of the B-related background, and the parameters of the $q\bar{q}$ background float in the fit. We find 12263 ± 168 fully reconstructed B mesons. The B signal region is defined by requiring $M(B)$ to be within 30–40 MeV/c^2 (depending on the B decay mode) of the nominal B mass.

Reconstructed B^+ or $\bar{B}^0$ candidates are combined with π^-'s–the right-sign (RS) combination–and the missing mass $M_{\mathrm{miss}}(B\pi)$ is calculated as $M_{\mathrm{miss}}(B\pi) = \sqrt{(\sqrt{s} - E_{B\pi})^2/c^4 - P_{B\pi}^2/c^2}$, where $E_{B\pi}$ and $P_{B\pi}$ are the measured energy and momentum of the reconstructed $B\pi$ combination. Signal $e^+e^- \to BB^*\pi$ events produce a narrow peak in the $M_{\mathrm{miss}}(B\pi)$ spectrum around the nominal B^* mass while $e^+e^- \to B^*B^*\pi$ events produce a peak at $m_{B^*} + \Delta m_{B^*}$, where $\Delta m_{B^*} = m_{B^*} - m_B$, due to the missed photon from the $B^* \to B\gamma$ decay. It is important to note here that, according to signal MC simulations, $BB^*\pi$ events, where the reconstructed B is the one from the B^*, produce a peak in the $M_{\mathrm{miss}}(B\pi)$ distribution at virtually the same
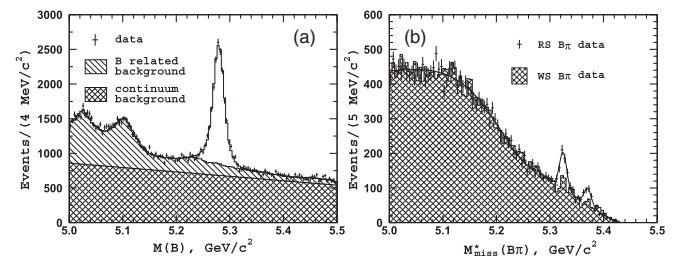

FIG. 1. (a) Invariant mass and (b) $M_{\mathrm{miss}}^*(B\pi)$ distribution for B candidates in the B signal region. Points with error bars represent the data. The open histogram in (a) shows the result of the fit to data. The solid line in (b) shows the result of the fit to the RS $B\pi$ data; the dashed line represents the background level.

position as $BB^*\pi$ events, where the reconstructed B is the primary one. To remove the correlation between $M_{\mathrm{miss}}(B\pi)$ and $M(B)$ and to improve the resolution, we use $M^*_{\mathrm{miss}} = M_{\mathrm{miss}}(B\pi) + M(B) - m_B$ instead of $M_{\mathrm{miss}}(B\pi)$. The M^*_{miss} distribution for the RS combinations is shown in Fig. 1(b), where peaks corresponding to the $BB^*\pi$ and $B^*B^*\pi$ signals are evident. Combinations with π^+—the wrong-sign (WS) combinations—are used to evaluate the shape of the combinatorial background. (The $B \to J/\psi K^0$ mode is not included in the WS sample, but both combinations with π^+ and π^- are added to the RS sample.) We apply a factor of 1.19 ± 0.01 [12] to the WS distribution to normalize it to the expected number of the background events in the RS sample. There is also a hint for a peaking structure in the WS M^*_{miss} distribution, shown as a hatched histogram in Fig. 1(b). Because of $B^0 - \bar{B}^0$ oscillations, we expect a fraction of the produced B^0 mesons to decay as $\bar{B}^0$ given by $0.5x_d^2/(1 + x_d^2) = 0.1861 \pm 0.0024$, where x_d is the B^0 mixing parameter [11].

Note that the momentum spectrum of B mesons produced in events with initial-state radiation (ISR), $e^+e^- \to \gamma B\bar{B}$, overlaps significantly with that for B mesons from the three-body $e^+e^- \to B^{(*)}B^{(*)}\pi$ processes. However, ISR events do not produce peaking structures in the M^*_{miss} distribution.

A binned maximum likelihood fit is performed to fit the M^*_{miss} distribution to the sum of three Gaussian functions to represent three possible signals and two threshold components $A_k(x_k - M^*_{\mathrm{miss}})^{\alpha_k} \exp\{(M^*_{\mathrm{miss}} - x_k)/\delta_k\}$ $(k = 1, 2)$ to parametrize the $q\bar{q}$ and two-body $B^{(*)}\bar{B}^{(*)}$ backgrounds. The means and widths of the signal Gaussian functions are fixed from the signal MC simulation. The parameters A_k, α_k, δ_k of the background functions are free parameters of the fit; the threshold parameters x_k are fixed from the generic MC simulations. ISR events produce an M^*_{miss} distribution similar to that for $q\bar{q}$ events; these two components are modeled by a single threshold function. The resolution of the signal peaks in Fig. 1(b) is dominated by the c.m. energy spread and is fixed at 6.5 and 6.2 MeV/c^2 for the $BB^*\pi$ and $B^*B^*\pi$, respectively as determined from the signal MC simulations. The fit to the RS spectrum yields $N_{BB\pi} = 13 \pm 25$, $N_{BB^*\pi} = 357 \pm 30$, and $N_{B^*B^*\pi} = 161 \pm 21$ signal events. The statistical significance of the observed $BB^*\pi$ and $B^*B^*\pi$ signal is 9.3σ and 8.1σ, respectively. The statistical significance is calculated as $\sqrt{-2\ln(\mathcal{L}_0/\mathcal{L}_{\mathrm{sig}})}$, where $\mathcal{L}_{\mathrm{sig}}$ and $\mathcal{L}_0$ denote the likelihood values obtained with the nominal fit and with the signal yield fixed at zero, respectively.

For the subsequent analysis, we require $|M^*_{\mathrm{miss}} - m_{B^*}| < 15$ MeV/c^2 to select $BB^*\pi$ signal events and $|M^*_{\mathrm{miss}} - (m_{B^*} + \Delta m_B)| < 12$ MeV/c^2, where $\Delta m_B = m_{B^*} - m_B$, to select $B^*B^*\pi$ events. For the selected $B^{(*)}B^*\pi$ candidates, we calculate $M_{\mathrm{miss}}(\pi) = \sqrt{(\sqrt{s} - E_\pi)^2/c^4 - P_\pi^2/c^2}$, where E_π and P_π are the reconstructed energy and momentum, respectively, of the charged pion in the c.m.
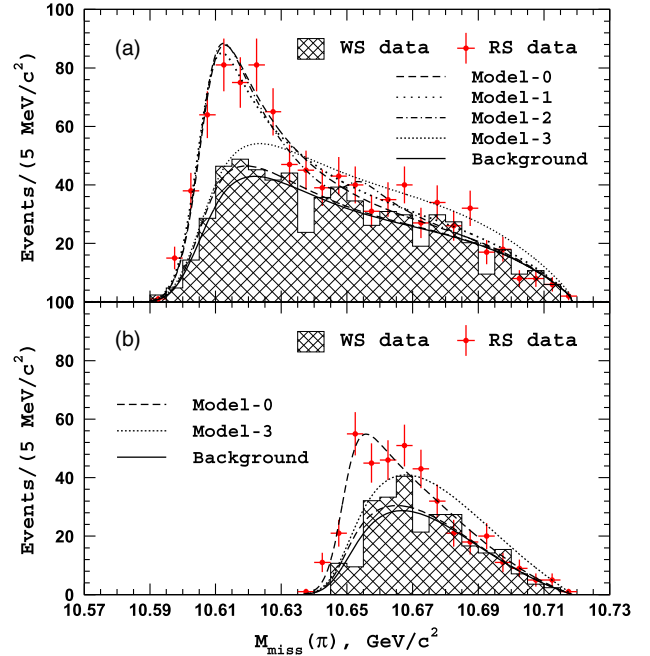

FIG. 2. The $M_{\mathrm{miss}}(\pi)$ distribution for the (a) $BB^*\pi$ and (b) $B^*B^*\pi$ candidate events. Normalization factor is applied for the WS distributions.

frame. The $M_{\mathrm{miss}}(\pi)$ distributions are shown in Fig. 2 [13]. We perform a simultaneous binned maximum likelihood fit to the RS and WS samples, assuming the same number (after normalization) and distribution of background events in both samples and known fraction of signal events in the RS sample that leaks to the WS sample due to mixing. To fit the $M_{\mathrm{miss}}(\pi)$ spectrum, we use the function

$$F(m) = [f_{\mathrm{sig}}S(m) + B(m)]\epsilon(m)F_{\mathrm{PHSP}}(m), \quad (1)$$

where $m \equiv M_{\mathrm{miss}}(\pi)$, $f_{\mathrm{sig}} = 1.0$ $(0.1366 \pm 0.0032$ [14]) for the RS (WS) sample, $S(m)$ and $B(m)$ are the signal and background probability density function, respectively, and $F_{\mathrm{PHSP}}(m)$ is the phase space function. To account for the instrumental resolution, we smear the function $F(m)$ with a Gaussian function with $\sigma = 6.0$ MeV/c^2 that is dominated by the c.m. energy spread. The reconstruction efficiency is parametrized as $\epsilon(m) \sim \exp[(m - m_0)/\Delta](1 - m/m_0)^{3/4}$, where $m_0 = 10.718 \pm 0.001$ GeV/c^2 is an efficiency threshold and $\Delta = 0.094 \pm 0.002$ GeV/c^2.

The distribution of background events is parametrized as $B_{B^{(*)}B^*\pi}(m) = b_0 e^{-\beta\delta_m}$, where b_0 and β are fit parameters and $\delta_m = m - (m_{B^{(*)}} + m_{B^*})$. A general form of the signal probability density function is written as

$$S(m) = |\mathcal{A}_{Z_b(10610)} + \mathcal{A}_{Z_b(10650)} + \mathcal{A}_{\mathrm{nr}}|^2, \quad (2)$$

where $\mathcal{A}_{\mathrm{nr}} = a_{\mathrm{nr}}e^{i\phi_{\mathrm{nr}}}$ is the nonresonant amplitude parametrized as a complex constant and the two Z_b amplitudes,

$\mathcal{A}_{Z_b}$, are parametrized with Breit-Wigner functions $\mathcal{A}_{Z_b} = a_Z e^{i\phi_Z}/(m^2 - m_Z^2 - i\Gamma_Z m_Z)$. The masses and widths of the Z_b states are fixed at the values obtained from the analyses of $e^+e^- \to \Upsilon(nS)\pi^+\pi^-$ and $e^+e^- \to h_b(mP)\pi^+\pi^-$: $M_{Z_b(10610)} = 10607.2 \pm 2.0 \, \text{MeV}/c^2$, $\Gamma_{Z_b(10610)} = 18.4 \pm 2.4 \, \text{MeV}$ and $M_{Z_b(10650)} = 10652.2 \pm 1.5 \, \text{MeV}/c^2$, $\Gamma_{Z_b(10650)} = 11.5 \pm 2.2 \, \text{MeV}$ [1].

We first analyze the $BB^*\pi$ [$B^*B^*\pi$] data with the simplest hypothesis, model 0, which includes only the $Z_b(10610)$ [$Z_b(10650)$] amplitude. Results of the fit are shown in Fig. 2; the numerical results are summarized in Table I. The fraction f_X of the total three-body signal attributed to a particular quasi-two-body intermediate state is calculated as $f_X = \int |\mathcal{A}_X|^2 dm / \int S(m) dm$, where $\mathcal{A}_X$ is the amplitude for a particular component X of the three-body amplitude. Next, we extend the hypothesis to include a possible nonresonant component, model 1, and repeat the fit to the data. Then the $BB^*\pi$ data are fit to a combination of two Z_b amplitudes, model 2. In both cases, the addition of an extra component to the amplitude does not give a statistically significant improvement in the data description: the likelihood value is only marginally improved (see Table I). The addition of extra components to the amplitude also produces multiple maxima in the likelihood function. As a result, we use model 0 as our nominal hypothesis. Finally, we fit both samples to a pure nonresonant amplitude (model 3). In this case, the fit is significantly worse.

If the parameters of the Z_b resonances are allowed to float, the fit to the $BB^*\pi$ data with model 0 gives $10605 \pm 6 \, \text{MeV}/c^2$ and $25 \pm 7 \, \text{MeV}$ for the $Z_b(10610)$ mass and width, respectively, and the fit to the $B^*B^*\pi$ data gives $10648 \pm 13 \, \text{MeV}/c^2$ and $23 \pm 8 \, \text{MeV}$ for the $Z_b(10650)$ mass and width, respectively. The large errors here reflect the strong correlation between the resonance parameters.

The three-body Born cross sections are calculated as

$$\sigma(e^+e^- \to f) = \frac{N_f}{L\mathcal{B}_f \alpha \eta (1 + \delta_{\text{ISR}})|1 - \Pi|^2}, \qquad (3)$$

where N_f is the three-body signal yield and $L = 121.4 \, \text{fb}^{-1}$ is the total integrated luminosity. The efficiency-weighted sum of B-meson branching fractions $\mathcal{B}_f$ is determined using both signal MC and two-body $e^+e^- \to B^{(*)}\bar{B}^{(*)}$ events in data. To avoid the large systematic uncertainties associated with the determination of reconstruction efficiencies for B and D decays to multibody final states, we select a subset of two-body modes, $B^+ \to \bar{D}^0[K^+\pi^-]\pi^+$ and $B \to J/\psi[\ell^+\ell^-]K$, and calculate $\mathcal{B}_f = \mathcal{B}_f^{\text{sel}} \times N_{B^{(*)}\bar{B}^{(*)}}^{\text{all}}/N_{B^{(*)}\bar{B}^{(*)}}^{\text{sel}}$, where the superscripts "sel" and "all" refer to quantities determined for the selected subset of B decay modes and for the full set of modes, respectively. Two-body $e^+e^- \to B^{(*)}\bar{B}^{(*)}$ events are selected with the requirement $0.90 < P(B) < 1.35 \, \text{GeV}/c$; the B yield is determined from the fit to the $M(B)$ distribution. We find $N_{B^{(*)}\bar{B}^{(*)}}^{\text{all}} = 10131 \pm 152$ and $N_{B^{(*)}\bar{B}^{(*)}}^{\text{sel}} = 2406 \pm 62$. (MC studies show no significant dependence of the reconstruction efficiency on the B momentum.) To account for the nonuniform distribution of signal events over the phase space, we introduce an efficiency correction factor η determined from the MC simulation with signal events generated according to the nominal model. Since we do not observe a signal in the $BB\pi$ final state, no correction is made for this channel. A factor $\alpha = 0.897 \pm 0.002$ is introduced to correct for the effect of neutral B-meson oscillations that is determined using the known B^0 mixing parameter x_d and the yield ratio in data of two-body events with a reconstructed neutral versus charged B meson. The ISR correction, $1 + \delta_{\text{ISR}}$, for the $B^{(*)}B^*\pi$ final states is calculated using recent results on $\sigma(e^+e^- \to h_b(mP)\pi^+\pi^-)$ [15] and an observation that the $\Upsilon(5S) \to h_b(mP)\pi^+\pi^-$ transitions are saturated by the intermediated Z_b production [1]; for the $BB\pi$ final state we assume constant cross section. For the vacuum polarization correction we use $1/|1 - \Pi|^2 = 0.928$ [16]. The results are summarized in Table II.

The dominant sources of systematic uncertainties for the three-body production cross sections are the uncertainties

TABLE I. Summary of fit results to the $M_{\text{miss}}(\pi)$ distributions for the three-body $BB^*\pi$ and $B^*B^*\pi$ final states.

| Mode | Parameter | Model 0 | Model 1 | | Model 2 | | Model 3 |
			Solution 1	Solution 2	Solution 1	Solution 2	
$BB^*\pi$	$f_{Z_b(10610)}$	1.0	1.45 ± 0.24	0.64 ± 0.15	1.01 ± 0.13	1.18 ± 0.15	$\cdots$
	$f_{Z_b(10650)}$	$\cdots$	$\cdots$	$\cdots$	0.05 ± 0.04	0.24 ± 0.11	$\cdots$
	$\phi_{Z_b(10650)}$, radians	$\cdots$	$\cdots$	$\cdots$	-0.26 ± 0.68	-1.63 ± 0.14	$\cdots$
	f_{nr}	$\cdots$	0.48 ± 0.23	0.41 ± 0.17	$\cdots$	$\cdots$	1.0
	ϕ_{nr}, radians	$\cdots$	-1.21 ± 0.19	0.95 ± 0.32	$\cdots$	$\cdots$	$\cdots$
	$2\log\mathcal{L}$	-304.7	-300.6	-300.5	-301.4	-301.4	-344.5
$B^*B^*\pi$	$f_{Z_b(10650)}$	1.0	1.04 ± 0.15	0.77 ± 0.22			$\cdots$
	f_{nr}	$\cdots$	0.02 ± 0.04	0.24 ± 0.18			1.0
	ϕ_{nr}, radians	$\cdots$	0.29 ± 1.01	1.10 ± 0.44			$\cdots$
	$2\log\mathcal{L}$	-182.4	-182.4	-182.4			-209.7

TABLE II. Summary of results on three-body cross sections. The first (or sole) uncertainty is statistical, the second is systematic.

Parameter	$BB\pi$	$BB^*\pi$	$B^*B^*\pi$
N_f, events	13 ± 25	357 ± 30	161 ± 21
$\mathcal{B}_f$, 10^{-6}	293 ± 22	276 ± 21	223 ± 17
η	1.0	1.066	1.182
$1 + \delta_{\text{ISR}}$	0.720 ± 0.017	0.598 ± 0.016	0.594 ± 0.016
σ, pb	< 2.9	$17.4 \pm 1.6 \pm 1.9$	$8.75 \pm 1.15 \pm 1.04$

in the signal yield extraction (6.9% for $BB^*\pi$ and 8.7% for $B^*B^*\pi$), in the reconstruction efficiency (7.6%) (including secondary branching fractions [11]), in the correction factor α (1%), in the integrated luminosity (1.4%), and in the ISR correction (2.7%). The overall systematic uncertainties for the three-body cross sections are estimated to be 7.9%, 10.8%, and 12.0% for the $BB\pi$, $BB^*\pi$, and $B^*B^*\pi$ final states, respectively.

Using the results of the fit to the $M_{\text{miss}}(\pi)$ spectra with the nominal model (model 0 in Table I) and the results of the analyses of $e^+e^- \to \Upsilon(nS)\pi^+\pi^-$ [1] and $e^+e^- \to h_b(mP)\pi^+\pi^-$ [15,17], we calculate the ratio of the branching fractions $\mathcal{B}[Z_b^+(10610) \to \bar{B}^0B^{*+} + B^+\bar{B}^{*0}]/\mathcal{B}[Z_b^+(10610) \to \text{bottomonium}] = 5.93^{+0.99+1.01}_{-0.69-0.73}$ and $\mathcal{B}[Z_b^+(10650) \to B^{*+}\bar{B}^{*0}]/\mathcal{B}[Z_b^+(10650) \to \text{bottomonium}] = 2.80^{+0.69+0.54}_{-0.40-0.36}$. We also calculate the relative fractions for Z_b decays, assuming that they are saturated by the already observed $\Upsilon(nS)\pi$, $h_b(mP)\pi$, and $B^{(*)}B^*$ channels. The results are presented in Table III.

To summarize, we report the first observations of the three-body $e^+e^- \to BB^*\pi$ and $e^+e^- \to B^*B^*\pi$ processes with a statistical significance above 8σ. Measured Born cross sections are $\sigma(e^+e^- \to [B\bar{B}^* + \text{c.c.}]^\pm\pi^\mp) = (17.4 \pm 1.6 \pm 1.9)$ pb and $\sigma(e^+e^- \to [B^*\bar{B}^*]^\pm\pi^\mp) = (8.75 \pm 1.15 \pm 1.04)$ pb. For the $e^+e^- \to BB\pi$ process, we set a 90% confidence level upper limit of $\sigma(e^+e^- \to$

$[B\bar{B}]^\pm\pi^\mp) < 2.9$ pb. The analysis of the $B^{(*)}B^*$ mass spectra indicates that the total three-body rates are dominated by the intermediate $e^+e^- \to Z_b(10610)^\mp\pi^\pm$ and $e^+e^- \to Z_b(10650)^\mp\pi^\pm$ transitions for the $BB^*\pi$ and $B^*B^*\pi$ final states, respectively.

TABLE III. B branching fractions for the $Z_b^+(10610)$ and $Z_b^+(10650)$ decays. The first quoted uncertainty is statistical, the second is systematic.

Channel	Fraction, %	
	$Z_b(10610)$	$Z_b(10650)$
$\Upsilon(1S)\pi^+$	$0.54^{+0.16+0.11}_{-0.13-0.08}$	$0.17^{+0.07+0.03}_{-0.06-0.02}$
$\Upsilon(2S)\pi^+$	$3.62^{+0.76+0.79}_{-0.59-0.53}$	$1.39^{+0.48+0.34}_{-0.38-0.23}$
$\Upsilon(3S)\pi^+$	$2.15^{+0.55+0.60}_{-0.42-0.43}$	$1.63^{+0.53+0.39}_{-0.42-0.28}$
$h_b(1P)\pi^+$	$3.45^{+0.87+0.86}_{-0.71-0.63}$	$8.41^{+2.43+1.49}_{-2.12-1.06}$
$h_b(2P)\pi^+$	$4.67^{+1.24+1.18}_{-1.00-0.89}$	$14.7^{+3.2+2.8}_{-2.8-2.3}$
$B^+\bar{B}^{*0} + \bar{B}^0B^{*+}$	$85.6^{+1.5+1.5}_{-2.0-2.1}$	$\cdots$
$B^{*+}\bar{B}^{*0}$	$\cdots$	$73.7^{+3.4+2.7}_{-4.4-3.5}$

[1] A. Bondar *et al.* (Belle Collaboration), Phys. Rev. Lett. **108**, 122001 (2012).

[2] A. Garmash *et al.* (Belle Collaboration), Phys. Rev. D **91**, 072003 (2015).

[3] D.-Y. Chen and X. Liu, Phys. Rev. D **84**, 094003 (2011); A. Ali, C. Hambrock, and W. Wang, Phys. Rev. D **85**, 054011 (2012); I. V. Danilkin, V. D. Orlovsky, and Y. A. Simonov, Phys. Rev. D **85**, 034012 (2012); S. Ohkoda, Y. Yamaguchi, S. Yasui, K. Sudoh, and A. Hosaka, Phys. Rev. D **86**, 014004 (2012); E. Braaten, C. Langmack, and D. H. Smith, Phys. Rev. D **90**, 014044 (2014).

[4] A. E. Bondar, A. Garmash, A. I. Milstein, R. Mizuk, and M. B. Voloshin, Phys. Rev. D **84**, 054010 (2011).

[5] A. Drutskoy *et al.* (Belle Collaboration), Phys. Rev. D **81**, 112003 (2010).

[6] A. Abashian *et al.* (Belle Collaboration), Nucl. Instrum. Methods Phys. Res., Sect. A **479**, 117 (2002); also see Detector section in J. Brodzicka *et al.*, Prog. Theor. Exp. Phys. **2012**, 04D001.

[7] S. Kurokawa and E. Kikutani, Nucl. Instrum. Methods Phys. Res., Sect. A **499**, 1 (2003), and other papers included in this volume; T. Abe *et al.*, Prog. Theor. Exp. Phys.**2013**, 03A001and following articles up to 03A011.

[8] D. J. Lange, Nucl. Instrum. Methods Phys. Res., Sect. A **462**, 152 (2001).

[9] R. Brun *et al.*, CERN Report No. DD/EE/84-1, 1984.

[10] D. Liventsev *et al.* (Belle Collaboration), Phys. Rev. D **77**, 091503(R) (2008).

[11] K. A. Olive *et al.* (Particle Data Group Collaboration), Chin. Phys. C **38**, 090001 (2014).

[12] Determined from the requirement of equal number of events in the RS and WS samples in the $5.0 < M^*_{\text{miss}} < 5.24$ GeV/c^2 region in the data.

[13] See Supplemental Material at http://link.aps.org/supplemental/10.1103/PhysRevLett.116.212001 for the bin-by-bin information.

[14] Determined using mixing parameter x_d and the ratio of charged to neutral B yields measured in data from two-body $e^+e^- \to B^{(*)}\bar{B}^{(*)}$ processes. Renormalization factor of 1.19 ± 0.01 is also applied.

[15] A. Abdesselam *et al.* (Belle Collaboration), arXiv: 1508.06562.

[16] S. Actis *et al.*, Eur. Phys. J. C **66**, 585 (2010).

[17] The fits to the $M_{\mathrm{miss}}(\pi)$ distributions performed in Ref. [1] give fractions of $f_{Z(10610)^{\pm}\pi^{\mp}} = 0.423^{+0.05+0.007}_{-0.127-0.009}$ $(0.352^{+0.156+0.001}_{-0.004-0.134})$ and $f_{Z(10650)^{\pm}\pi^{\mp}} = 0.602^{+0.103+0.11}_{-0.211-0.038}$ $(0.648^{+0.152+0.067}_{-0.114-0.155})$ for the $h_b(1P)$ [$h_b(2P)$] decays.